Self-Suppression of Signal-Signal Beating Interference using a Split-Carrier Transmitter

Thomas Gerard[1]* , Zhixin Liu[1], Lidia Galdino[1], Polina Bayvel[1] and Domaniç Lavery[1]

[1]*Optical Networks Group, Dept. of Electronic & Electrical Engineering, University College London, London, UK*
*E-mail: uceetmh@ucl.ac.uk

Keywords: Point-to-Point Optical Transmission, Digital Signal Handling Techniques

Abstract

A transmitter-side carrier tone is applied to suppress SSBI in a 112 Gb/s double sideband IM/DD system using a split-carrier transmitter. This novel, low-complexity approach achieves comparable performance to a computationally-intensive linearised receiver without any additional opto-electronic hardware or linearisation DSP.

1   Introduction

Low complexity, single polarisation direct-detection links represent the most pragmatic transmission scheme for networks with a large number of point-to-point connections, such as metro and intra-datacentre networks. When transmitting spectrally-efficient, Nyquist-shaped subcarrier modulation (N-SCM) quadrature amplitude modulation (QAM) data, performance is limited by the square-law response of the receiving photodiode, which is the source of signal-signal beating interference (SSBI) [1]. The mitigation of SSBI through linearisation digital signal processing (DSP) has been a field of intense research, offering signal-to-noise ratio (SNR) gains of 4 dB and higher [2–5]. Of these, the Kramers-Kronig receiver is seen as a particularly promising solution for >100 Gb/s/λ links [6–8]. However, these methods are often computationally intensive, such that recent research has focused on simplification of the DSP [9]. Alternatively, SSBI cancellation using optical hardware has been proposed [10, 11]. For instance, it has been shown that by applying a powerful carrier tone at the receiver, SSBI can be suppressed without any linearisation DSP [12]. However, these methods can require polarisation management as well as additional optical sources and photodiodes.

The recently proposed split-carrier transmitter (SCT) offers an effective solution to this problem as it applies the carrier tone at the transmitter side, in contrast with [12]. By routing a portion of the transmission laser power around a modulator before recombining, a powerful, polarisation- and phase-matched carrier tone is added to the signal with minimal hardware modifications. In previous work this system has been highlighted for its ability to reduce modulation loss [13]. In this paper, the effectiveness of using the SCT transmitter-side carrier tone to suppress SSBI is investigated. This was done by measuring the SCT performance with carrier-to-signal power ratio (CSPR) in simulation and experiment. This determined how much power should be routed around the modulator as the strong external carrier, suppressing SSBI. This process was then repeated using a DSP-linearised receiver, allowing the inherent SSBI-suppression of the DSP-free SCT to be quantified in comparison.

2   Principle of SSBI suppression

The ideal split-carrier transmitter is shown in Fig. 1. A continuous wave (CW) laser source is split into two arms at coupler C1. The lower arm is modulated, while the upper arm is unchanged. These arms are then immediately recombined at coupler C2. This results in a high power, polarisation- and phase-matched carrier tone that is coupled with the modulated signal. This can all be achieved with a photonic integrated circuit, requiring no additional opto-electronic hardware. The coupling ratio of C1 and C2 determine both the optical loss across the SCT as well as the CSPR. These are calculated simply by considering the coupling losses of C1 and C2 together, and are shown in Fig. 1. In this plot, the carrier coupling coefficient refers to the fraction of power routed through the carrier branch by C1 and C2 (assumed identical). As the carrier coupling coefficient is increased the overall transmitter loss decreases and the CSPR increases. This is the root of the SCT's ability to self-suppress SSBI: by raising the carrier coupling coefficient, the SSBI is reduced due to the high CSPR, while the optical power at the receiver is simultaneously increased.
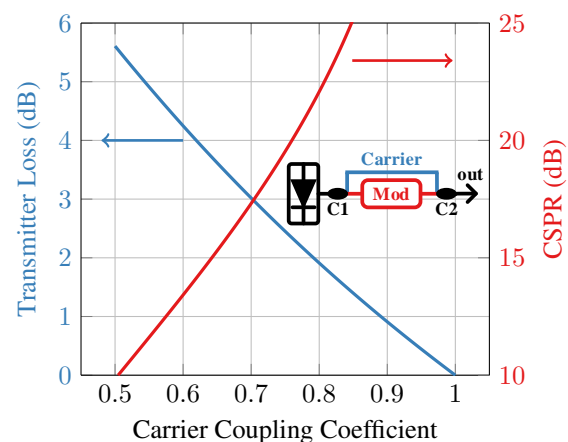

Fig. 1 Relationship between the carrier coupling coefficient, the CSPR and the loss across the split-carrier transmitter, for a typical dynamic modulator loss of 10 dB.
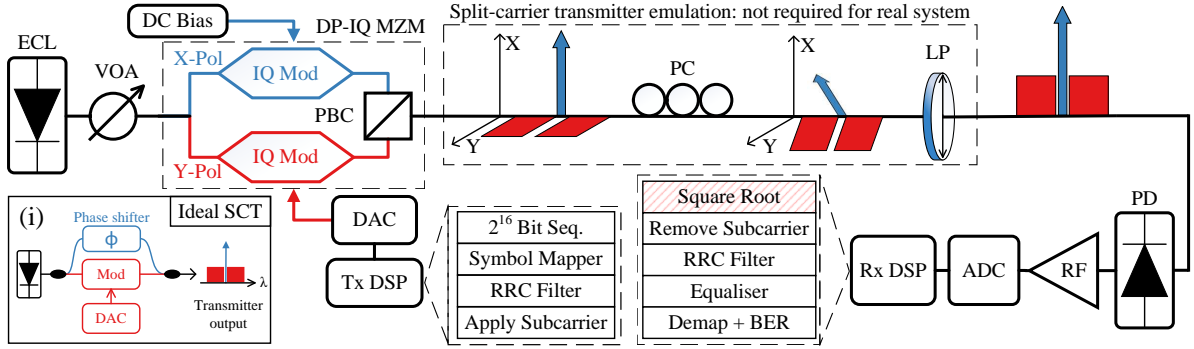
Fig. 2 Experimental configuration used to emulate an integrated SCT. Note that the ideal SCT design does not require a PC or LP; see in inset (i). The square root is not part of the proposed system, and is only used for comparison with a linearised receiver.

3 Methodology

3.1 Experimental Configuration

The experimental setup was designed to emulate an integrated SCT. An external cavity laser (ECL) with a 100 kHz linewidth emitting at 1552 nm was coupled into a dual-polarisation (DP)-IQ Mach Zehnder modulator (MZM), as shown in Fig. 2. Data was applied to the Y-polarisation (Pol) IQ modulator, biased at its null-point, while the X-Pol IQ modulator was biased to maximise the carrier power. This way, the X-Pol serves as the carrier branch of the SCT while the Y-Pol acts as a typical modulator. To restore the carrier and the data to the same polarisation, a polarisation controller (PC) followed by a linear polariser (LP) with an extinction ratio of 30 dB was used. To set the CSPR, the PC was rotated to control the proportion of carrier and signal tones allowed through the LP. This was measured using an optical spectrum analyser (OSA).

A 92 GS/s digital to analogue converter (DAC) with a 3 dB bandwidth of 28 GHz was used for signal generation. Both inputs of the Y-Pol IQ modulator were driven with the same 28 GBd 16QAM N-SCM signal. This created a real valued, double sideband (DSB) signal. A DSB signal was chosen due to its inherent ability to cancel SSBI-induced phase interference, permitting linearisation using a simple square root receiver [14]. This is not a requirement of the SCT, which works with any modulation format. After the LP, the recombined signal was passed to a single-ended PIN photodiode, forming an intensity modulated, direct detection (IM/DD) link. The electrical signal was radio frequency (RF) amplified by 17 dB and digitised using an 8 bit analogue to digital converter (ADC) with a 3 dB bandwidth of 33 GHz.

The DSP used to generate the N-SCM is also shown in Fig. 2. A 2^{16} De Bruijn sequence was mapped to 16QAM symbols before being Nyquist-shaped using a root raised cosine (RRC) filter with a roll off factor of 0.01. The baseband signal was digitally upconverted using a subcarrier frequency of 15.75 GHz, resulting in a subcycle ratio of $15.75/28 = 0.5625$, defined as the subcarrier frequency divided by the symbol rate (selected for experimental convenience). At the receiver-side, the signal was normalised, then optionally linearised by applying a square root to the signal. The signal was then downconverted using

a second digital 15.75 GHz clock tone. The baseband signal was match filtered and resampled to two samples per symbol. A 21-tap decision-directed constant modulus algorithm (CMA) equaliser was used for data recovery before the symbols were demapped and passed to a bit error rate (BER) estimator.

3.2 Simulation Procedure

A simulation of the SCT was also performed. This was carried out in Matlab by implementing the DSP steps listed in Fig. 2. Monte Carlo methods were used to measure BER vs received power. Shot and thermal noise were modelled at the photodiode using a dark current of 10 nA and a device temperature of 298 K. An experimentally measured responsivity of 0.55 A/W was considered. Thermal noise equivalent to the RF amplifier's 6 dB noise figure was also included [15]. For an accurate system performance prediction, SNR vs OSNR was experimentally measured and the implementation penalty compared to the theoretical prediction was included in the simulation.
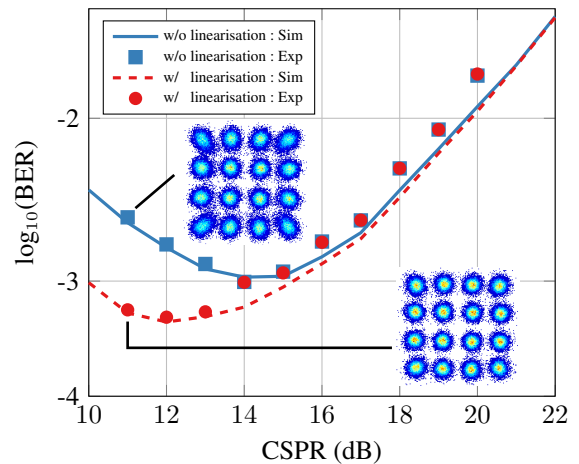
4 Results

4.1 Fixed Received Power

Fig. 3 Simulated and experimental performance of the SCT with CSPR for a received power of -3 dBm. The constellations show how SSBI is corrected for by a square root receiver.

The performance of the SCT for a received power of -3 dBm (selected arbitrarily) is shown in Fig. 3 with and without linearisation. For accurate performance prediction, the linearised simulation was calibrated using the experimental data point at a CSPR of 12 dB. As expected, the linearised signal shows significant improvement in the low CSPR regime, with the optimum CSPR decreasing from 14 to 12 dB. This represents a direct gain for a standard transmitter, which typically seeks to minimize CSPR [7]. However, this is not the case for the SCT, for which transmission loss decreases as CSPR increases (Fig. 1). To account for this, the SCT results must also be assessed for a fixed CW power, accounting for both link-loss as well as receiver performance.

4.2 Fixed CW Power

Fig. 4 shows the SCT performance for a fixed CW power. BER as a function of CSPR is presented with and without linearisation DSP. It was not possible to vary the internal coupling coefficient of the DP-IQ MZM used in this experiment, therefore, only simulation results are presented. A CW power of 0.5 dBm was considered, selected for comparable performance with Fig. 3 at a CSPR of 14 dB. A range of carrier coupling coefficients were considered, thereby varying both the transmitter loss and the CSPR (see Fig. 1).

As shown in Fig. 4, the linearised receiver provided only modest improvement at the optimum CSPR, where the BER was reduced by 32%. This can be explained by noting that the optimum CSPR for both the standard and linearised receivers is 15 dB. This contrasts with the fixed received power case shown in Fig. 3, where the optimum CSPRs are 12 and 14 dB. This is significant, as it shows that the SCT benefits more by raising the CSPR, and hence reducing transmission loss, than it does by reducing the CSPR and exploiting the gains made by the linearised receiver. In this way the SCT shows it can self-suppress SSBI, as its optimum CSPR is one in which transmitter noise dominates, rather than SSBI. These limiting regimes are overlaid on Fig. 3.
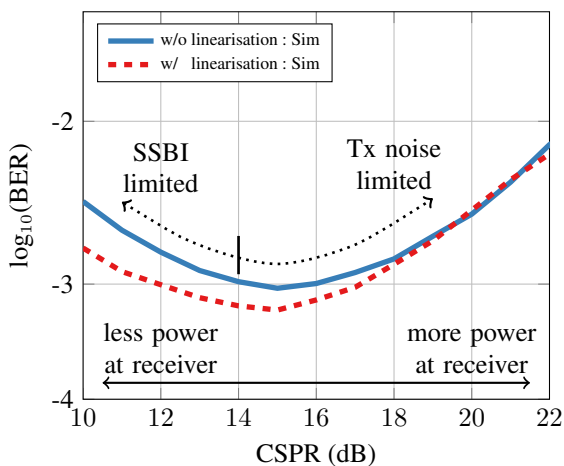

Fig. 4 Simulated performance of the SCT with CSPR for a fixed CW power of 0.5 dBm. The optimum CSPR of 15 dB is transmitter noise limited, regardless of linearisation.

To quantify the performance of the standard and linearised receivers, the fixed CW power simulation was repeated for a range of CW powers. The optimum BER for each curve was plotted against CW power, shown as lines in Fig. 5. To supported this simulation, experimental data similar that shown in Fig. 3 was taken for received optical powers of -6 to -2 dBm in integer steps. For each curve, the linearised simulation was fitted to the real data by eye to better inform the CW power simulation. These points are plotted as markers.
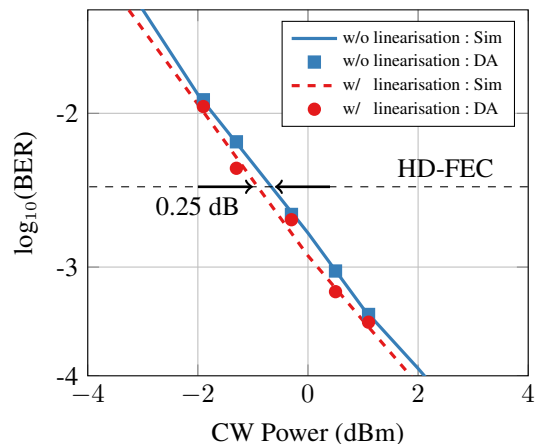

Fig. 5 Back to back SCT performance vs available CW power, with and without receiver linearisation DSP. DA: data aided.

Also overlaid on Fig. 5 is the hard decision forward error correction (HD-FEC) threshold corresponding to a BER 3.8×10^{-3}. At this level the difference between the standard and linearised SCT is measured as just 0.25 dB. This demonstrates the effectiveness of the standard SCT in suppressing SSBI, as complete removal of SSBI offers only small gains. The SCT is therefore shown to effectively self-suppress SSBI without any additional DSP or opto-electronic hardware.

5 Conclusion

A 112 Gb/s double sideband IM/DD split-carrier transmitter was used to self-suppress SSBI without computationally intensive linearisation DSP or additional opto-electronic hardware, for the first time. The laser source was split then recombined after modulation, creating a powerful transmitter-side carrier tone. By correctly setting the split-ratio, the SCT can approach the performance of a DSP-linearised receiver to within 0.25 dB. This demonstrates the effectiveness of the standard SCT to self-suppress SSBI. This simple method is modulation format independent, and shows the SCT to be a promising low-complexity solution for IM/DD datacentre links.

6 Acknowledgements

7 References

[1] Lowery, A.J., 'Amplified-spontaneous noise limit of optical OFDM lightwave systems', Optics Express, **16**, (2), pp. 860-865, 2008, DOI:10.1364/OE.16.000860

[2] Peng, W., Wu, X., Feng, K., et al., 'Spectrally efficient direct-detection OFDM transmission employing an iterative estimation and cacellation technique', Optics Express, **17**, (11), pp. 9099-9111, 2009, DOI:10.1364/OE.17.009099

[3] Li, Z., Erkılınç, M.S., Pachnicke, S., et al., 'Signal-signal beat interference cancellation in spectrally-efficient WDM direct-detection Nyquist-pulse-shaped 16-QAM subcarrier modulation', Optics Express, **23**, (18), pp. 23694-23709, 2015, DOI:10.1364/OE.23.023694

[4] Randel, S., Pilori, D., Chandrasekhar, S., et al., '100-Gb/s discrete-multitone modulation with novel interference-cancellation scheme', Proc. Eur. Conf. Opt. Commun., 2015, Paper no. Mo.4.5.2

[5] Li, Z., Erkılınç, M.S., Maher, R., et al., 'Two-stage linearization filter for direct-detection subcarrier modulation', IEEE Photonics Technology Letters, **28**, (24), pp. 2838-2841, 2016, DOI:10.1109/LPT.2016.2623491

[6] Mecozzi, A., Antonelli, C., Shtaif, M., 'Kramers-Kronig coherent receiver', Optica, **3**, (11), pp 1220-1227, 2016, DOI:10.1364/OPTICA.3.001220

[7] Li, Z., Erkılınç, M.S., Shi, K., et al., 'Digital Linearization of Direct-Detection Transceivers for Spectrally Efficient 100 Gb/s/λ WDM Metro Networking', Jounral of Lightwave Technology, **36**, (1), pp 27-36, 2018, DOI:10.1109/JLT.2017.2777858

[8] Chen, X., Antonelli, A., Chandrasekhar S., et al., '218-Gb/s single-wavelength, single-polarization, single-photodiode transmission over 125-km of standard single-mode fiber using Kramers-Kronig detection', Proc. Conf. Opt. Fiber Commun., 2017, Paper no. Th5B.6

[9] Bo, T., Kim, H., 'Kramers-Kronig recevier operable without digital upsampling', Optics Express, **26**, (11), pp. 13810-13818, 2018, DOI:10.1364/OE.26.013810

[10] Peng, W., Morita, I., Tanaka, H., 'Enabling high capacity direct-detection opitcal OFDM transmissions using beat interference cancellation receiver', Proc. Eur. Conf. Opt. Commun., 2010, Paper no. We.B3.2

[11] Nezamalhosseini, S.A., Chen, L., Zhuge, Q., et al., 'Theoretical and experimental investigation of direct detection optical OFDM transmission using beat interference cacellation receiver', Optics Express, **21**, (13), pp. 15237-15246, 2013, DOI:10.1364/OE.21.015237

[12] Corcoran, B., Foo, B., Lowery, A.J., 'Single-photodiode per polarization receiver with signal-signal beat interference suppression through heterodyne detection', Optics Express, **26**, (3), pp. 3075-3086, 2018, DOI:10.1364/OE.26.003075

[13] Gerard, T., Erkılınç, M.S., Liu, Z., et al., 'A low-loss split-carrier transmitter architecture for intra-datacentre communications', Proc. Eur. Conf. Opt. Commun., 2018

[14] Poggiolini P., Bosco, G., Benlachtar, Y., et al., 'Long-haul 10 Gbit/s linear and non-linear IMDD transmission over uncompensated standard fiber using a SQRT-metric MLSE receiver', Optics Express, **16**, (17), pp. 12919-12936, 2008, DOI:10.1364/OE.16.012919

[15] Agrawal, G., 'Fiber-Optic Communication Systems, 3rd Ed., John Wiley & Sons, 2002